EEET ECOLOGICAL ENGINEERING & ENVIRONMENTAL TECHNOLOGY

Ecological Engineering & Environmental Technology, 2026, 27(1), 325–335
https://doi.org/10.12912/27197050/215462
ISSN 2719–7050, License CC-BY 4.0

Received: 2025.11.23
Accepted: 2025.12.21
Published: 2026.01.01

Spatiotemporal distribution and risk assessment of polycyclic aromatic hydrocarbons in the Tigris River near Baghdad Medical City wastewater discharge

Omar Jasim Mohammed[1*], Mahmood Basil Mahmood[1]

[1] Biology Department, College of Science, University of Baghdad, Baghdad, Iraq
* Corresponding author's e-mail: jassem2402m@sc.uobaghdad.edu.iq

ABSTRACT

Polycyclic aromatic hydrocarbons (PAHs) are persistent, carcinogenic contaminants. We tracked the 16 U.S. Environmental Protection Agency (EPA) priority PAHs in surface waters of the Tigris River at five stations spanning 100 m upstream to 1.5 km downstream of Baghdad Medical City's wastewater outfall during October 2024, January 2025, and April 2025. Samples underwent liquid–liquid extraction (LLE), copper desulfurization, and gas chromatography with flame-ionization detector (GC-FID) analysis. Total PAH concentrations (Σ16 PAHs) peaked at the sewer outlet in all seasons (up to 31 µg L^{-1}) and declined at 1.5 km downstream to levels close to the pre-sewage discharge point. Site explained 93.75% of the spatiotemporal variance ($p < 0.001$). The share of high-molecular-weight PAHs rose from 48% at the outfall to 67% after 1.5 km. Total risk quotient (ΣRQ) peaked at 2.5×10^3 in January, exceeding the safety threshold, while benzo[a]pyrene-equivalent toxicity (BaP-TEQ) peaked at 1.9 µg BaP eq L^{-1}. Winter benzo[a]pyrene (0.262 µg L^{-1}) exceeded Dutch and Canadian aquatic criteria by 17–26-fold. Diagnostic ratios trace the origin of PAHs to medical waste and biomass combustion

Keywords: benzo[a]pyrene, biomass combustion, diagnostic ratios, polycyclic aromatic hydrocarbons, risk quotient, Tigris River, wastewater.

INTRODUCTION

The Tigris River, one of Iraq's two main rivers, flows through Baghdad City for approximately 60 km, mostly within urban areas (Asaad and Abed, 2020). Rapid urbanization, diffuse agricultural runoff, and chronically underperforming wastewater infrastructure have already driven several physicochemical parameters beyond Iraqi and World Health Organization (WHO) limits, signaling a steady decline in water quality (Grmasha et al., 2023). In large cities such as Mosul, up to 400,000 m^3 day^{-1} of untreated domestic, industrial, and hospital effluent are discharged daily into the Tigris River, severely burdening the river's ecological system and compromising water quality (Hmoshi et al., 2024). Due to a lack of proper guidelines and infrastructure, hospital waste is generally mixed with municipal waste, which makes segregation and disposal even more difficult and dangerous (Hassan and Mahmood, 2019; Al-Hiyaly et al., 2016). Consumption of substandard drinking water elevates population-level health risks and, consequently, escalates healthcare expenditures (Al-Dhamin, 2023). wastewater can be the source of aromatic compounds that can enter the river and pose risk to aquatic organisms (Ahmed et al., 2021). Polycyclic aromatic hydrocarbons (PAHs) are among the key aromatic organic pollutants found in both medical waste and municipal wastewater due to their widespread generation from incomplete combustion processes and organic chemical discharge (Patel et al., 2020; Kurwadkar et al., 2022). PAHs are divided into low-molecular-weight (LMW) with 2 to 3 benzene rings and 4 to 6 rings high-molecular-weight (HMW) based on their structure and properties (Hassan et al., 2019). Studies indicate that more toxic compounds can form from reactions of

low molecular weight PAHs with other pollutants, such as nitrated and oxy-PAHs (Peng et al., 2023). HMW PAHs are persistence in the environment, known to be associated with severe toxicological effects, including carcinogenicity and mutagenicity (Juda et al., 2019). Incomplete incineration of plastic-based medical supplies has increased the proportion of synthetic polymers, along with pharmaceutical formulations and laboratory solvents used in large hospital complexes, generating polycyclic aromatic hydrocarbons (PAHs), which are hydrophobic and carcinogenic compounds (Srivastava et al., 2024; Agarwal et al., 2024; Montano et al., 2025). PAHs are on the short list of substances for which all significant regulators worldwide have already established binding water limits due to clear evidence of genotoxicity and cancer risk. The Guidelines of the World Health Organization for Drinking Water Quality retain a health-based value of 0.7 μg L^{-1} for benzo[a]pyrene, the sentinel PAH used as a proxy for the group (WHO, 2022). The European Union's Water Framework Directive goes further: Directive 2013/39/EU identifies four harmful PAHs: benzo[a]pyrene (BaP), benzo[b] fluoranthene (BbF), benzo[k]fluoranthene (BkF), and indeno[1,2,3-cd]pyrene (Ind[1,2,3-cd]P) as important substances, setting a safe limit of 0.05 μg L^{-1} for BaP in rivers and lakes. The Safe Drinking Water Act in the United States sets a mandatory maximum contaminant level (MCL) of 0.2 μg L^{-1} for BaP and an MCL goal of zero (EP & CEU, 2013; U.S. EPA, 2024). Recent human studies show that greater daily PAH intake is associated with higher levels of BaP–DNA (BPDE) adducts, an established biomarker linked to cancer risk (Guo et al., 2024). Additionally, even minimal concentrations of BaP in water, such as 0.1 μg L^{-1}, caused developmental stress in some aquatic organisms (Xu et al., 2023). This study investigates the distribution and risks of polycyclic aromatic hydrocarbons (PAHs) along the Baghdad Medical City outfall transect. It measures all 16 EPA priority PAHs shown in Table 1, at five sampling points (–100 m, 0 m, +100 m, +500 m, +1500 m) across three seasons: autumn 2024, winter 2025, and spring 2025. Spatial and seasonal variations are evaluated using Kruskal–Wallis test, while a comprehensive set of diagnostic molecular ratios is applied to identify PAH sources and compare exposure levels with international health guidelines. Furthermore, ecological and human-health risks are assessed through the calculation of risk quotients (RQ) and toxic equivalency (TEQ) metrics.

Table 1. Abbreviations, full chemical names, and number of fused aromatic rings for the 16 U.S. EPA priority polycyclic aromatic hydrocarbons (PAHs) quantified in this study

Abbreviation	Full name	Number of rings
Nap	Naphthalene	2
Acy	Acenaphthylene	3
Ace	Acenaphthene	3
Flu	Fluorene	3
Phe	Phenanthrene	3
Ant	Anthracene	3
Flt	Fluoranthene	4
Pyr	Pyrene	4
BaA	Benz[a]anthracene	4
Chr	Chrysene	4
BbF	Benzo[b]fluoranthene	5
BkF	Benzo[k]fluoranthene	5
BaP	Benzo[a]pyrene	5
IcdP	Indeno[1,2,3-cd]pyrene	6
DBA	Dibenzo[a,h]anthracene	5
BghiP	Benzo[ghi]perylene	6

MATERIALS AND METHODS

Study area and sampling sites

Baghdad Medical City is a 3.000-bed healthcare complex in Baghdad, Iraq (33°20′49″ N, 44°22′44″ E. that releases mixed hospital wastewater through an underground gravity conduit directly into the Tigris River. Moreover, multiple investigations have shown that this untreated discharge elevates heavy metal loads (Abd Al-Satar and Sachit, 2021). and microbial indicators (Oleiwi and Al-Dabbas, 2022), within the first few hundred meters downstream of the outfall. Five sampling stations were therefore established along the thalweg, as summarized in Table 2: a control 100 m upstream of the outfall (S1, -100 m); the effluent pipe itself (S2); and three downstream points (S3, +100 m), (S4, +500 m), and (S5, +1500 m). to minimize bank-side bias and ensure adequate grab sampling depth, all sites were mid-channel (~15 m from either bank) except for S2 in which the sampling was directly from the effluent pipe. Figure 1 shows Study area Map and Sampling Sites.

Sampling design

Water was collected during three seasons: October 2024, January 2025, and April 2025. At

each station, Grab samples were collected at 50cm depth using 1 L amber borosilicate glass bottles. Bottles were pre-cleaned following APHA Standard Methods: washed with laboratory-grade detergent, rinsed with deionized water, and flushed with acetone and n-hexane to eliminate organic residue (Lee et al., 2023; Baird et al., 2017). Bottles were air-dried, sealed with ground-glass stoppers, and rinsed three times with site water before sampling. To minimize oxidative loss of polycyclic aromatic hydrocarbons (PAHs), samples were collected without agitation, leaving no air headspace, and dosed in situ with sodium thiosulfate at a concentration of 80 mg L^{-1} (ISO, 2024).

Laboratory analysis

Water samples were processed within seven days of collection using a liquid–liquid extraction method (Chen et al., 2019). An aliquot of 100 mL homogenized water sample was transferred into a clean glass tube and mixed with 30 mL of a mixture of acetone and n-hexane (1:1, v/v). The mixture was vortexed for 1 minute and subjected to ultrasonic treatment for 15 minutes to enhance phase contact and extraction efficiency. Samples were centrifuged for 10 minutes at 3000 rpm to separate the organic phase from the aqueous phase. The upper organic phase was collected with a Pasteur pipette, and the aqueous phase was re-extracted twice with 10 mL portions of acetone: n-hexane (1:1). All organic extracts were combined, treated with activated copper to remove elemental sulfur, and dried over anhydrous sodium sulfate. The eluate was further concentrated to 1mL using the rotary evaporator, transferred to amber GC vials, and subsequently refrigerated at 4 °C before analysis. The investigation was conducted at the laboratories of the Ministry of Science and Technology, at the Food Research Centre, Baghdad /Iraq, using a Shimadzu GC-2010 gas chromatograph (Japan).

Quality control

External standard techniques were used to establish the quantitative standards for the 16 PAHs present in the water sample. The linearity correlation for 16 PAHs was 0.997. Analyte concentration was used to determine the limits of detection (LOD), which were then calculated using a three-fold signal-to-noise ratio (Zhang et al., 2022). The LOD range for water was 0.06 µg L^{-1}. Each sample was tested in triplicate using a method blank (solvent), a spiked blank (standards added to solvent), and a sample. There was no discernible PAH contamination, as indicated by method blank analysis.

RESULTS AND DISCUSSION

Overview

Sixteen PAH congeners were quantified at all five stations in October 2024, January 2025, and April 2025. Concentrations of the summed 16 compounds (Σ16PAH) shown in Table 3, ranged from 3.52 µg L^{-1} at the upstream background (S1, January) to 30.98 µg L^{-1} at the Medical-City wastewater outfall (S2, January). Although lower than the historic Shatt Al-Hilla spike 602 µg L^{-1} (Hussein et al., 2014), and peaks of 327 and 279 µg L^{-1} by (Zaki et al., 2025), and (Al-Azawii et al., 2015), respectively. this value still places the Medical-City outfall among the highest BaP records for Iraqi freshwaters and signals chronic ecological risk. The winter maximum of benzo[a]pyrene at S2 0.262 µg L^{-1} exceeds the Dutch negligible concentration criterion 0.010 µg L^{-1} by 26 x and the Canadian Council of Ministers of the Environment (CCME) aquatic life guideline 0.015 µg L^{-1} by 17 x. A one-way ANOVA revealed a highly significant spatial variation in total PAHs among the five sampling sites ($F_{4,10} = 37.57$, p

Table 2. Geographic coordinates and spatial distribution of sampling sites along the Tigris River near Baghdad Medical City

Sites	Site description	Longitude	Latitude
Site-1	500 m upstream of the discharge point	44°22′19.0″E	33°21′05.8″N
Site-2	Discharge point	44°22′22.2″E	33°20′52.1″N
Site-3	100 m downstream	44°22′19.7″E	33°20′47.9″N
Site-4	500 m downstream	44°22′25.1″E	33°20′37.3″N
Site-5	1500 m downstream	44°23′01.5″E	33°20′28.2″N

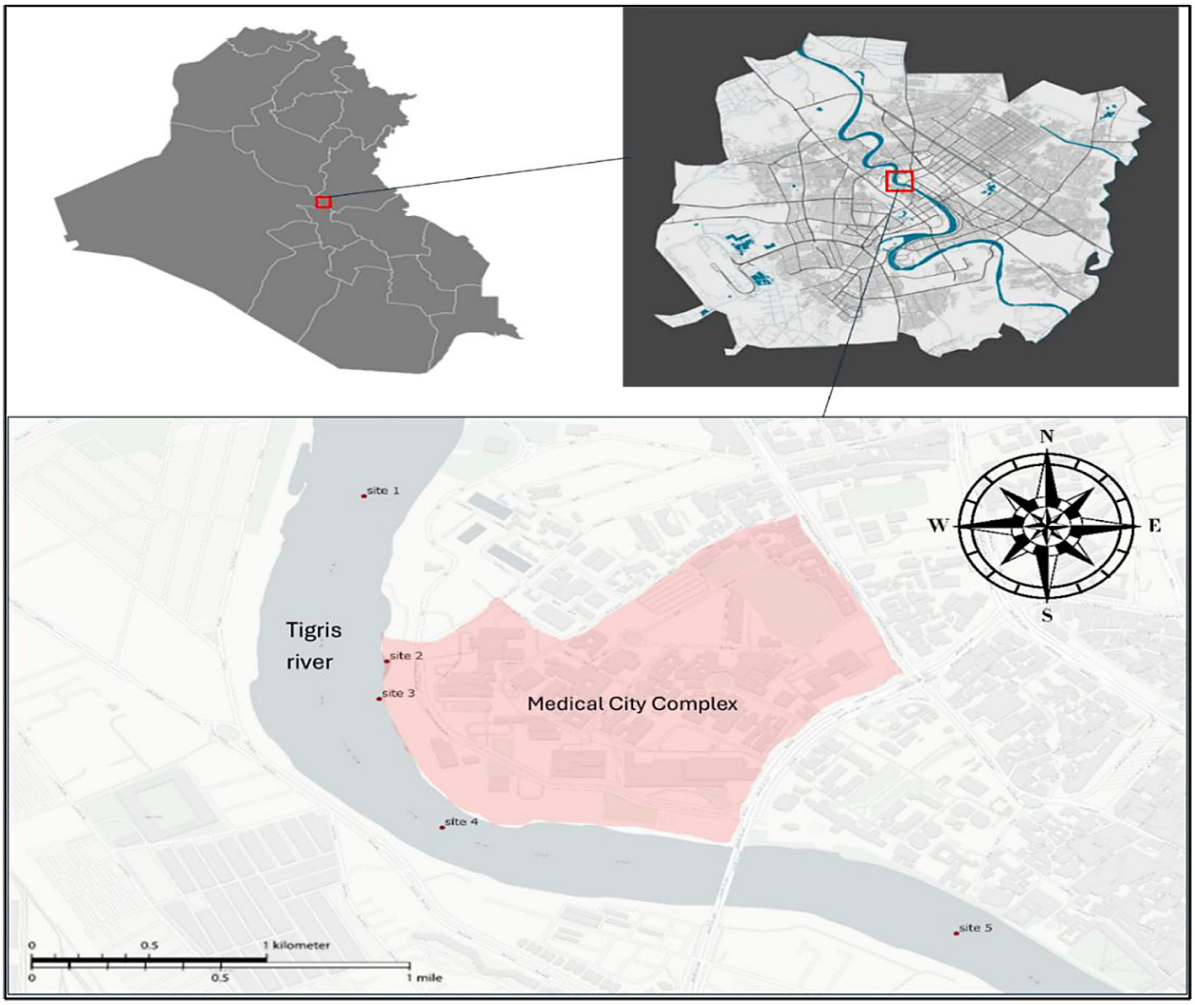

Figure 1. Study area map showing Baghdad Medical City and five PAH sampling sites along the Tigris River. Inset maps show the location of the study area within Baghdad and Iraq. SAGA GIS (Version 9.7.1) https://saga-gis.sourceforge.io

< 0.001). Post-hoc Tukey HSD analysis showed that Site 2 exhibited the highest total PAH concentration (28.17 µg/L), significantly exceeding all other sites ($p < 0.001$). Site 3 (17.83 µg/L) was also significantly higher than Sites 1, 4, and 5, indicating that elevated PAH levels persist for at least 100 m downstream of the discharge. Sites 1 (4.75 µg/L) and 5 (9.17 µg/L) formed the lowest homogeneous subset, representing background or recovered water quality conditions. Site 4 (11.53 µg/L) was positioned within an intermediate subset with moderate contamination. The spatial pattern followed the order S1 < S5 < S4 < S3 < S2, confirming the strong localized impact of the hospital effluent and partial downstream recovery. Homogeneous subset analysis supported this pattern, grouping S1 and S5 as low-PAH sites, S4 as moderate, and S3 and S2 as highly contaminated.

Spatial patterns

Site S2, located at the effluent outfall, was the dominant hot spot in every season, with Σ16PAH concentrations four to six-fold higher than those at the control S1 (23.58 vs 4.04 µg L^{-1} in October, 30.98 vs 3.52 µg L^{-1} in January, and 30.1 vs 6.69 µg L^{-1} in April). Approximately 100 m downstream, S3 recorded the second-highest values (15.62–21.84 µg L^{-1}), indicating rapid yet incomplete dilution of the wastewater. Stations S4 and S5, situated 500–1500 m downstream, carried intermediate loads of about 8.06–11.9 µg L^{-1}, still two to three times the rural background. This persistent spatial hierarchy S2 >> S3 > S4 ≈ S5 > S1, shows that proximity to the wastewater outlet, rather than season, governs absolute PAH concentrations in the reach. Across the five stations, a clear longitudinal shift from low to high-molecular-weight dominance emerges.

Seasonal patterns

Mean concentrations of Σ16 PAH rose slightly from October (12.9 μg L^{-1}) to January (13.8 μg L^{-1}) and April (16.2 μg L^{-1}). The outfall station (S2) displayed a clear winter maximum (30.9 μg L^{-1}) with negligible spring decline, reflecting sustained effluent input. Immediately downstream (S3) concentrations were lowest in January (15.6 μg L^{-1}) and 35% higher in April. The upstream control (S1) and far-field site (S5) likewise showed winter minima (3.52 and 8.06 μg L^{-1}) and spring maxima (6.69 and 10.4 μg L^{-1}), whereas the mid-reach station (S4) remained nearly constant (~11–12 μg L^{-1}). Central-Baghdad reaches (urban Tigris) show winter maxima, driven by domestic heating (Mustafa et al., 2023). while cleaner rural tributaries often peak in spring due to reduced dilution.

Composition of the 16 priority PAHs

LMW/HMW variation in the water column

Because molecular weight governs solubility and breakdown rates, PAHs follow a predictable environmental pattern. Low molecular weight (2–3 ring) congeners stay relatively water soluble and are quickly lost through volatilization and microbial breakdown (Berríos-Rolón et al., 2025). High molecular weight (4–6 rings) PAHs, by contrast, are poorly soluble, less volatile, and more resistant to biodegradation; they sorb to particles and persist in river water and sediments even after LMW fractions have dissipated (Zhao et al., 2022). Spatial gradient based on annual means. By taking the mean values of HMW and LMW of all sites for each season as shown in Figure 2, the averaged Σ16PAH at S1 is still slightly enriched in LMW compounds (53.8% of Σ16PAH, 2.56 μg L^{-1} on average), and at the Medical City outfall (S2), the profile is similar (LMW 52.78 %, 14.9 μg L^{-1}). Just 100 m downstream (S3), the balance tips as HMW species rise to 58% of the total and remain the controlling fraction further downstream, climbing to 64 % at S4 and 67% at S5. In absolute terms, the LMW load collapses by almost 80% between S2 (14.9 μg L^{-1}) and S5 (3.0 μg L^{-1}), whereas the HMW pool is only halved, from 13.3 → 6.1 μg L^{-1}. Together with the concurrent drop in Σ16PAH concentrations 28 → 9 μg L^{-1}, this pattern indicates that lighter, more volatile and biodegradable PAHs are preferentially lost during river transport, while 4–6 ring congeners persist and progressively dictate the mixture's toxic potential downstream. Seasonal shifts. Comparing according to seasonal variations, the LMW/HMW ratio at (S1) is always near parity yet trends slightly toward LMW in spring. LMW climbs from 52.7% (Oct) and 50.8% (Jan) to 56% (Apr). At S2, composition is remarkably constant, LMW hovers at 52 ± 1% across all dates, even though the total mass peaks in January (31 μg L^{-1}) and remains high in April. The source signature, therefore, appears stable and largely immune to seasonal hydrology. At S3, the January column still shows strong HMW dominance (62%), but by April the profile has flattened (HMW ≈ 50%), driven by a two-fold rise in LMW load (10.94 μg L^{-1}). Farther downstream at S4 and S5, the winter snapshot (Jan) is the most HMW skewed of the year (70.8% at S4 and 73% at S5). With spring flows, however, the balance swings: LMW shares jump to 45.1% (S4) and 43.1% (S5) in April, cutting the HMW dominance by about 20 percentage points while total PAH drops only modestly. High HMW shares are frequently linked to pyrogenic inputs such as diesel generators, incineration of clinical waste, and heavy traffic, whereas petrogenic releases tend to elevate LMW and 4-ring PAHs (Janneh et al., 2023).

Source identification of PAHs

Diagnostic ratios were benchmarked against source-specific cut-off bands (Tobiszewski and Namieśnik, 2012). which classify PAH origins as petrogenic, vehicular, or biomass combustion without site-specific calibration, Table 4 shows the diagnostic-ratio ranges. The ring-class pattern reveals two dominant regimes: S2 (Medical City outfall) and S3 are consistently pyrogenic, while S1 shows a petrogenic background signal. S4 and S5 exhibit mixed signatures, shifting from pyrogenic in winter to more petrogenic in spring. At S2, all seasons fall within the combustion domain, with winter Ant/(Ant + Phe) = 0.20–0.63, Flu/(Flu + Pyr) = 0.28–0.56, and BaA/(BaA + Chr) = 0.42–0.56.Across stations, combustion dominates, but seasonal fingerprints vary. S1 shows low Flu/(Flu + Pyr) (<0.4) and Ant/(Ant + Phe) >0.10 in October–January, shifting toward combustion by April (Flu > 0.40). S2 and S3 remain unambiguously pyrogenic, with Flu/(Flu + Pyr) >0.50 and BaA/(BaA + Chr) >0.35, while IcdP/(IcdP + BghiP)

Table 3. Descriptive statistics (mean ± SD; range) for polycyclic aromatic hydrocarbon (PAH) concentrations (μg L^{-1}) measured at Sites 1–5 along the study reach

PAHs		Site 1	Site 2	Site 3	Site 4	Site 5
Nap	Mean ± SD	0.58 ± 0.18	5.54 ± 0.39	2.98 ± 0.72	1.09 ± 0.22	0.70 ± 0.31
	(Min-Max)	0.41 – 0.82	4.94 – 6.11	2.22 – 4.09	0.76 – 1.33	0.44 – 1.16
Acy	Mean ± SD	0.47 ± 0.19	1.89 ± 0.22	1.18 ± 0.21	0.54 ± 0.12	0.52 ± 0.16
	(Min-Max)	0.31 – 0.74	1.55 – 2.20	0.87 – 1.42	0.42 – 0.72	0.39 – 0.75
Ace	Mean ± SD	0.38 ± 0.26	2.05 ± 0.42	0.92 ± 0.30	0.81 ± 0.03	0.46 ± 0.24
	(Min-Max)	0.20 – 0.74	1.54 – 2.62	0.60 – 1.33	0.77 – 0.84	0.29 – 0.81
Flu	Mean ± SD	0.39 ± 0.13	1.60 ± 0.26	0.65 ± 0.21	0.51 ± 0.22	0.40 ± 0.11
	(Min-Max)	0.27 – 0.59	1.25 – 1.94	0.48 – 0.95	0.30 – 0.81	0.28 – 0.57
Phe	Mean ± SD	0.53 ± 0.07	1.89 ± 0.25	0.98 ± 0.54	0.89 ± 0.25	0.66 ± 0.16
	(Min-Max)	0.43 – 0.62	1.57 – 2.25	0.57 – 1.76	0.63 – 1.21	0.51 – 0.90
Ant	Mean ± SD	0.22 ± 0.14	1.93 ± 1.23	0.79 ± 0.69	0.32 ± 0.24	0.28 ± 0.13
	(Min-Max)	0.12 – 0.42	0.33 – 3.19	0.31 – 1.79	0.15 – 0.66	0.18 – 0.47
Flt	Mean ± SD	0.31 ± 0.09	2.57 ± 0.38	2.24 ± 0.38	1.04 ± 0.23	0.88 ± 0.35
	(Min-Max)	0.21 – 0.44	2.04 – 3.04	1.76 – 2.76	0.83 – 1.40	0.60 – 1.40
Pyr	Mean ± SD	0.63 ± 0.06	1.14 ± 0.15	0.76 ± 0.06	0.73 ± 0.04	0.66 ± 0.06
	(Min-Max)	0.56 – 0.73	0.93 – 1.32	0.70 – 0.86	0.68 – 0.80	0.58 – 0.75
BaA	Mean ± SD	0.17 ± 0.05	0.72 ± 0.07	0.48 ± 0.03	0.30 ± 0.05	0.28 ± 0.07
	(Min-Max)	0.10 – 0.24	0.65 – 0.86	0.45 – 0.52	0.23 – 0.37	0.20 – 0.38
Chr	Mean ± SD	ND	0.92 ± 0.26	0.56 ± 0.26	0.45 ± 0.12	0.38 ± 0.10
	(Min-Max)		0.58 – 1.21	0.36 – 0.92	0.35 – 0.63	0.27 – 0.55
BbF	Mean ± SD	0.39 ± 0.24	1.88 ± 0.84	1.08 ± 0.57	0.71 ± 0.21	0.57 ± 0.40
	(Min-Max)	0.22 – 0.74	0.77 – 2.73	0.62 – 1.89	0.53 – 1.02	0.29 – 1.15
BkF	Mean ± SD	0.25 ± 0.11	1.25 ± 0.43	0.85 ± 0.34	0.51 ± 0.04	0.20 ± 0.16
	(Min-Max)	0.11 – 0.38	0.66 – 1.67	0.55 – 1.36	0.46 – 0.59	0.08 – 0.43
BaP	Mean ± SD	ND	0.21 ± 0.06	0.14 ± 0.03	0.10 ± 0.01	0.11 ± 0.002
	(Min-Max)		0.13 – 0.27	0.11 – 0.18	0.09 – 0.12	0.11 – 0.113
IcdP	Mean ± SD	0.17 ± 0.10	1.79 ± 0.13	1.74 ± 0.41	1.40 ± 0.89	1.22 ± 0.90
	(Min-Max)	0.03 – 0.27	1.61 – 1.98	1.21 – 2.34	0.22 – 2.27	0.03 – 2.00
DBA	Mean ± SD	0.43 ± 0.18	1.59 ± 0.19	1.51 ± 0.24	1.29 ± 0.32	1.03 ± 0.21
	(Min-Max)	0.25 – 0.61	1.31 – 1.75	1.18 – 1.75	0.84 – 1.63	0.75 – 1.32
BghiP	Mean ± SD	ND	1.25 ± 0.09	1.01 ± 0.08	0.91 ± 0.07	0.86 ± 0.07
	(Min-Max)		1.10 – 1.39	0.91 – 1.12	0.79 – 1.00	0.76 – 0.95

Note: *ND indicates concentrations below the analytical detection limit

>0.55 indicates high-temperature sources (Wild et al., 1992; Cao et al., 2020). At S4 and S5, October ratios show BaA/(BaA + Chr) >0.35 (0.48–0.55) and IcdP/(IcdP + BghiP) >0.50, though Flu/(Flu + Pyr) remains petrogenic (0.33–0.37). January presents a similar mix, with Flu <0.40, indicating dilution of combustion residues. In April, IcdP collapses to 0.20 (S4) and 0.03 (S5), signaling a petroleum pulse, while Flu surges to 0.46–0.53 and BaA holds at 0.28–0.29, reflecting petroleum combustion. Overall, unburned oil inputs in spring partly mask but do not erase the persistent pyrogenic signature exported from the Medical City outfall.

Risk assessment

Risk quotient

The Iraqi Quality Standards. take a minimalist approach as they bundle all dissolved and particulate hydrocarbons under a single blanket cap of 10 μg L^{-1}.and only set an 0.7 μg L^{-1} limit for Benzo[a]pyrene (COSQC, 2009). Most national frameworks still leave big holes. EPA's National

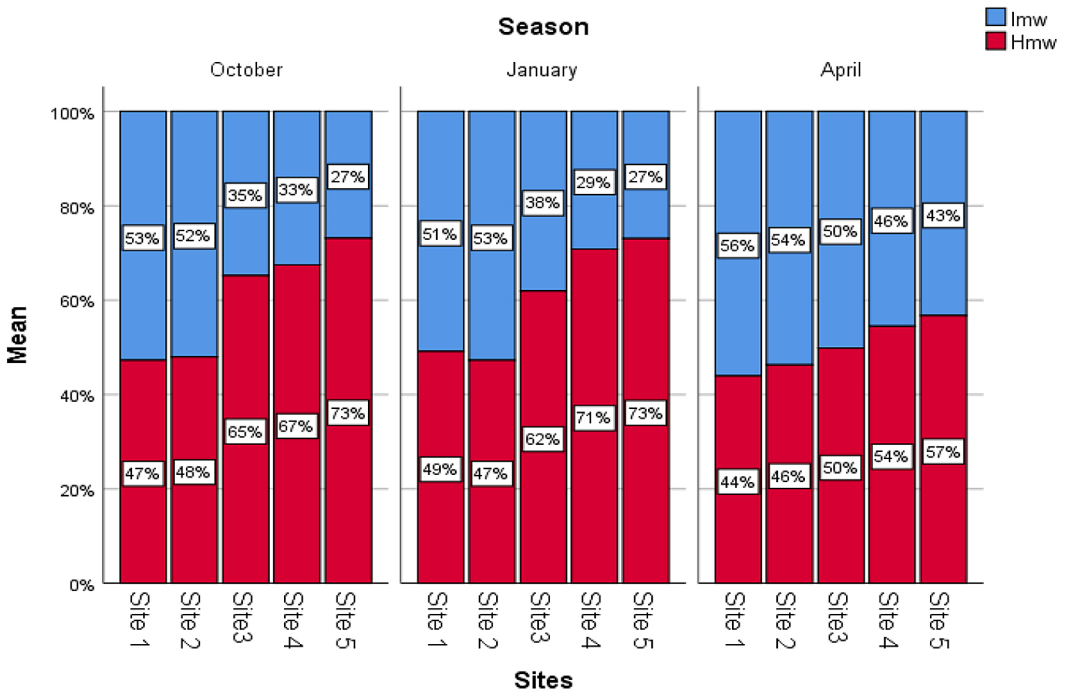

Figure 2. Percentage of LMW and HMW PAHs at the five sites during October, January, and April

Table 4. Characteristic diagnostic-ratio ranges for identifying PAH sources

Diagnostic ratio	Petrogenic	Fuel combustion	Pyrogenic and biomass burning
Ant / (Ant + Phe)	< 0.1	> 0.1	–
Flu / (Flu + Pyr)	< 0.4	0.4–0.5	> 0.5
BaA / (BaA + Chr)	< 0.2	> 0.35	0.2–0.35
IcdP / (IcdP + BghiP)	< 0.2	0.2–0.5	> 0.5

Recommended Water Quality Criteria publishes human-health thresholds for just 12 of the 16 priority PAHs (U.S. EPA, 2024). and Canada's CCME freshwater guidelines cover only 9 of them (CCME, 1999). In contrast, the Dutch National Institute for Public Health and the Environment, in its 2012 Report, National Institute for Public Health and the Environment (RIVM) sets compartment-specific MPC values for all 16 congeners (RIVM, 2012), which are routinely used when a complete ecological benchmark set is needed. These values represent chronic effect thresholds below which no long-term adverse ecological effects are expected. The risk quotient (RQ) is a screening-level metric used to estimate the potential ecological risk of a contaminant. It is calculated as the ratio of the measured environmental concentration (MEC_i) to the maximum permissible concentration (MPC_i) for the same compound. Table 5 shows interpretation of risk quotient (RQ_i) values.

For each compound and sample:

$$RQi = \frac{MECi}{MPCi} \quad (1)$$

where: RQ_i – risk quotient for compound i, MEC_i (µg/L) – measured environmental concentration of compound i in surface water, MPC_i (µg/L) – maximum permissible concentration established for compound i, representing the chronic no-effect level for aquatic organisms.

Risk-quotient analysis reveals a pervasive and severe mixture effect across the study area: the summed RQ (ΣRQ) at every station consistently

Table 5. Interpretation of risk quotient values

RQ < 1	Low/no risk expected.
RQ ≥ 1	Potential chronic risk to aquatic life
Higher RQ values	Urgent attention required

Table 6. Mean risk quotient and toxic-equivalency assessment of individual PAHs in Tigris River water

PAHs	TEF	MPC	Oct.			Jan.			Apr.		
			Mean MPC RQ	Mean TEQ ng/l	%ΣTEQ	Mean MPC RQ	Mean TEQ ng/l	%ΣTEQ	Mean MPC RQ	Mean TEQ ng/l	%ΣTEQ
Nap	0.001	2	1.26	1.95	0.01	1.59	2	0.11	0.42	2.57	0.16
Acy	0.001	1.3	0.79	0.81	0.04	0.92	0.84	0.05	0.42	1.1	0.07
Ace	0.001	3.8	0.25	0.69	0.04	0.32	0.86	0.05	0.16	1.22	0.08
Flu	0.001	1.5	0.62	0.69	0.04	0.49	0.6	0.03	0.31	0.82	0.05
Phe	0.001	1.1	0.91	0.87	0.05	1.08	0.8	0.05	0.7	1.29	0.08
Ant	0.01	0.1	8.12	2.34	0.13	9.84	7.68	0.43	3.26	11.2	0.71
Flt	0.001	0.12	10.92	1.48	0.08	16.2	1.34	0.08	8.07	1.4	0.09
Pyr	0.001	0.023	35.83	0.77	0.04	36.43	0.79	0.04	30.17	0.79	0.05
BaA	0.1	0.012	33.33	42.6	2.29	41.17	37.6	2.12	23.17	37	2.36
Chr	0.01	0.07	4.43	4.17	0.22	9.29	5.02	0.28	5.97	8	0.51
BbF	0.1	1.3	54.35	53.2	2.86	70.82	88.4	4.99	38.71	137	8.72
BkF	0.1	0.93	33.53	45.6	2.45	55.76	53.8	3.04	18.35	83.6	5.32
BaP	1	0.01	8	112.7	6.06	14.8	162.3	9.16	8.6	159.5	10.15
IcdP	0.1	0.0027	311.1	167.8	9.02	665	147.4	8.32	424.4	79	5.03
DBA	1	0.0014	560	1415	76.08	1088	1252	70.68	794.2	1036	65.95
BghiP	0.01	0.0082	58.78	9.95	0.53	130.4	9.87	0.56	105.6	10.4	0.66

exceeds 100. Even the upstream reference site S1, fails to meet ecological safety, recording RQ > 1 for seven to ten individual PAHs in each sampling period. Spatial patterns implicate the wastewater outfall at S2 as the principal point source; this station displays the highest single compound and cumulative RQs, and critically elevated risk persists for more than 1500 m downstream. The toxicity profile is dominated by HMW, carcinogenic PAHs particularly (DBA), (IcdP), (BbF).

Benzo[a]pyrene_equivalent (TEQ) assessment

This approach quantifies the overall carcinogenic potency of the PAH mixture by converting each of the 16 measured congeners into a benzo[a]pyrene-equivalent concentration (TEQ). Concentrations of the 16 EPA-priority PAHs were multiplied by the toxic-equivalency factors (TEFs) (ATSDR, 2022). Summing the 16 products yielded a benzo[a]pyrene-equivalent concentration (ΣTEQ) for every sample. Seasonal means were obtained by averaging the five station values within each campaign (October 2024, January 2025 and April 2025) and are reported in Table 6. Across the three surveys, cumulative ΣTEQ peaked in October at 1.86 µg BaP eq L^{-1}, declined slightly to 1.77 µg BaP eq L^{-1} in January (–4.8%), and reached a minimum of 1.57 µg BaP eq L^{-1} in April (15.6%). In every season, the toxicity profile was dominated by high-molecular-weight congeners: DBA alone contributed 66–76% of ΣTEQ and posted mean risk quotients (RQs) of 560–1089, two to three orders of magnitude above its maximum permissible concentration. IcdP added a further 8–9% (RQs 311–666), while benzo[b] and benzo[k]fluoranthene together accounted for 5–9. LMW PAHs each contributed ≤ 0.2% of ΣTEQ despite forming up to 10% of the mass load. The slight winter rise in (IcdP) toxicity and the progressive decline in DBA's fractional dominance toward spring suggest an interplay of reduced photolysis with higher organic inputs during colder months and enhanced dilution or degradation later in the year. Overall, a handful of 4–6-rings PAHs drive more than 90% of the mixture's toxic potency, marking them as priority targets for future mitigation and monitoring efforts along the Tigris River.

CONCLUSIONS

This study provides a comprehensive assessment of (PAHs) contamination in the Tigris River near Baghdad Medical City across three seasonal seasons. The findings reveal that PAH concentrations at the discharge point and

downstream stations consistently exceed ecological and human health safety thresholds, particularly during October. The diagnostic ratios point to a dominant pyrogenic origin of contamination, while risk quotient and toxic equivalency evaluations highlight a persistent and serious ecological threat. These results underscore the urgent need for regulatory intervention, improved wastewater treatment, and continuous environmental monitoring in urban rivers impacted by hospital effluents.

REFERENCES

1. Abd Al-Satar NH, Sachit DE. (2021 Aug). The effect of hospital wastewater discharge of Medical City, Baghdad, on heavy metals concentration of the Tigris River. *Desalination and Water Treatment*. *230*, 252–8. https://doi.org/10.5004/dwt.2021.27414
2. Agarwal S, Saha H, Kaushik SV, Patil VM. (2024 Nov). Critical review of biomedical waste management for future pandemics: Pharmaceutical perspective. *ACS Chemical Health & Safety. 31*(6), 444–467. https://doi.org/10.1021/acs.chas.4c00067
3. Agency for Toxic Substances and Disease Registry (ATSDR). (2022 Apr 14). Guidance for calculating benzo(a)pyrene equivalents for cancer evaluations of polycyclic aromatic hydrocarbons (PAHs). Atlanta (GA): ATSDR. https://www.atsdr.cdc.gov/pha-guidance/resources/ATSDR-PAH-Guidance-508.pdf
4. Ahmed GS, Mahmood MB, ALTahir BM. (2021). Determination of aniline in wastewater by cloud point extraction followed by HPLC using 8-hydroxyquinoline as a derivatization agent. *Pollution Research*. *40*(4), 1255–63. https://www.envirobiotechjournals.com/PR/v40i42021/Poll%20Res-20.pdf
5. Al-Azawii LH, Nashaat MR, Al-Azzawi MN. (2015). Determination of polycyclic aromatic hydrocarbon (PAHs) in the Tigris River through Passing Baghdad Province. *Iraqi Journal of Science*. 1372–84. http://ijsmah.uobaghdad.edu.iq/index.php/eijs/article/view/10104
6. Al-Dhamin A. (2023). Evaluation of the quality of potable water in Al-Rusafa side, Baghdad, Iraq. *Revista Bionatura*. *8*(4), 1–10. https://doi.org/10.21931/RB/2023.08.04.53
7. Al-Hiyaly SAK, Ma'alah WN, Al-Azzawi MN. (2016). Evaluating the effects of Medical City wastewater on water quality of Tigris River. *Engineering and Technology Journal*. *34*(B3), 405–17. https://doi.org/10.30684/etj.34.3B.8
8. Asaad BI, Abed BS. (2020). Flow characteristics of Tigris River within Baghdad City during drought. *Journal of Engineering* (University of Baghdad). *26*(3), 77–92.https://doi.org/10.31026/j.eng.2020.03.07
9. Baird RB, Eaton AD, Rice EW, editors. Standard Methods for the Examination of Water and Wastewater. 23rd ed. Washington (DC): American Public Health Association, American Water Works Association, Water Environment Federation; 2017. 1796. https://www.standardmethods.org
10. Berríos-Rolón PJ, Cotto MC, Márquez F. (2025 Apr 20). Polycyclic Aromatic Hydrocarbons (PAHs) in Freshwater Systems: A Comprehensive Review of Sources, Distribution, and Ecotoxicological Impacts. *Toxics*. *13*(4), 321. https://doi.org/10.3390/toxics13040321
11. Canadian Council of Ministers of the Environment. Canadian water quality guidelines for the protection of aquatic life: Polycyclic aromatic hydrocarbons (PAHs). In: Canadian Environmental Quality Guidelines, 1999. Winnipeg: CCME; 1999. https://ccme.ca/en/res/polycyclic-aromatic-hydrocarbons-pahs-en-canadian-water-quality-guidelines-for-the-protection-of-aquatic-life.pdf
12. Chen C-F, Ju Y-R, Lim Y-C, Hsieh S-L, Tsai M-L, Sun P-P, Katiyar R, Chen C-W, Dong C-D. (2019 Jul 22). Determination of polycyclic aromatic hydrocarbons in sludge from water and wastewater treatment plants by GC-MS. *International Journal of Environmental Research and Public Health*. *16*(14), 2604. https://doi.org/10.3390/ijerph16142604
13. European Parliament and Council of the European Union. Directive 2013/39/EU of 12 August 2013 amending Directives 2000/60/EC and 2008/105/EC as regards priority substances in the field of water policy. *Official Journal of the European Union*. 2013 Aug 24; L 226:1–17. https://eur-lex.europa.eu/legal-content/EN/TXT/?uri=celex%3A32013L0039
14. Grmasha RA, Stenger-Kovács C, Bedewy BAH, Al-sareji OJ, Al-Juboori RA, Meiczinger M, Hashim KS. (2023). Ecological and human health risk assessment of polycyclic aromatic hydrocarbons (PAH) in Tigris River near the oil refineries in Iraq. *Environmental Research*. *227*, 115791. https://doi.org/10.1016/j.envres.2023.115791
15. Guo L, Zhang X, Li X, Wang K, Wang Y, Abulikemu A, et al. (2024 Aug). Polycyclic aromatic hydrocarbon and its adducts in peripheral blood: Gene and environment interaction among Chinese population. *Environment International*. 190, 108922. https://doi.org/10.1016/j.envint.2024.108922
16. Hassan DF, Mahmood MB. (2019 May 1). Using of iron oxide nanoparticles and application in the removing of heavy metals from sewage water. *Iraqi Journal of Science*. *60*(4), 732–8. https://www.ijs.uobaghdad.edu.iq/index.php/eijs/article/view/729

17. Hassan FM, Alobaidy AH, Salman JM, Abdulameer SH. (2019). Distribution of polycyclic aromatic hydrocarbons in water and sediments in the Euphrates River, Iraq. *Iraqi Journal of Science*. *60*(12), 2572–2582. https://doi.org/10.24996/ijs.2019.60.12.5
18. Hmoshi RM, AL-Saleem S, Mohammed MI. (2024). Assessment of natural and municipal liquid wastes discharged into the Tigris River in Mosul-Iraq. *Egyptian Journal of Aquatic Biology and Fisheries*. *28*(4), 617–26. https://doi.org/10.21608/ejabf.2024.369171
19. Hussein FH, Karam FF, Baqir SJ. (2014 Apr 28). Monitoring of polycyclic aromatic hydrocarbons in surface water of Shatt Al-Hilla River. *Asian Journal of Chemistry*. *26*(9), 2768–72. https://doi.org/10.14233/ajchem.2014.16800
20. International Organization for Standardization. ISO 5667-3:2024. *Water quality — Sampling — Part 3: Preservation and handling of water samples.* 6th ed. Geneva (CH): ISO; 2024 Mar. 66. https://www.iso.org/standard/82273.html
21. Iraqi Central Organization for Standardization and Quality Control. (2009). *Iraqi Standard of Drinking Water No. 417, second modification*. Baghdad: Central Organization for Standardization and Quality Control.
22. Janneh M, Qu C, Zhang Y, Xing X, Nkwazema O, Nyihirani F, et al. (2023 Mar 1). Distribution, sources, and ecological risk assessment of polycyclic aromatic hydrocarbons in agricultural and dumpsite soils in Sierra Leone. *RSC Advances*. *13*(11), 7102–16. https://doi.org/10.1039/D2RA07955K
23. Juda SA, Salah MM, Salman JM. (2019 Sep). Efficiency of green algae Chlorella vulgaris in remediation of polycyclic aromatic hydrocarbon (anthracene) from culture media. *Baghdad Science Journal*. *16*(3), Article 1. https://doi.org/10.21123/bsj.2019.16.3.0543
24. Kurwadkar S, Sethi SS, Mishra P, Ambade B. (2022). Unregulated discharge of wastewater in the Mahanadi River Basin: Risk evaluation due to occurrence of polycyclic aromatic hydrocarbons in surface water and sediments. *Marine Pollution Bulletin*. *179*, 113686. https://doi.org/10.1016/j.marpolbul.2022.113686
25. Lee CC, Lin BL, Huang YW, Hsu NS, Chang WH. (2023 Mar 15). Simultaneous determination of 24 congeners of 2- and 3-monochloropropanediol esters and 7 congeners of glycidyl esters using direct multi-residue analytical LC-MS/MS methods in various food matrices. *Journal of Food and Drug Analysis*. *31*(1), 55–72. https://doi.org/10.38212/2224-6614.3442
26. Montano L, Baldini GM, Piscopo M, Liguori G, Lombardi R, Ricciardi M, Esposito G, Pinto G, Fontanarosa C, Spinelli M, Palmieri I, Sofia D, Brogna C, Carati C, Esposito M, Gallo P, Amoresano A, Motta O. (2025 Feb 23). Polycyclic aromatic hydrocarbons (PAHs) in the environment: Occupational exposure, health risks and fertility implications. *Toxics*.13(3), 151. https://doi.org/10.3390/toxics13030151
27. Mustafa RA, Al-Rudainy AJ, Abbas LM. (2023 Feb 22). Detection the accumulation of polycyclic aromatic hydrocarbons (PAHs) in tissues of *Arabibarbus grypus* collected from Tigris river, Iraq. *Iraqi Journal of Agricultural Sciences*. *54*(1), 100–5. https://doi.org/10.36103/ijas.v54i1.1680
28. Oleiwi AS, Al-Dabbas M. (2022 Apr 8). Assessment of contamination along the Tigris River from Tharthar–Tigris Canal to Azizziyah, Middle of Iraq. *Water*. *14*(8), 1194. https://doi.org/10.3390/w14081194
29. Patel A, Shaikh S, Jain K, Desai C, Madamvar D. (2020 Nov). Polycyclic aromatic hydrocarbons: Sources, toxicity, and remediation approaches. *Frontiers in Microbiology*. *11*, 562813. https://doi.org/10.3389/fmicb.2020.562813
30. Peng B, Dong Q, Li F, Wang T, Qiu X, Zhu T. (2023 Sep 13). A systematic review of polycyclic aromatic hydrocarbon derivatives: occurrences, levels, biotransformation, exposure biomarkers, and toxicity. *Environmental Science & Technology*. *57*(41), 15314–35. https://doi.org/10.1021/acs.est.3c03170
31. Srivastava A, Sharma A, Jena MK, Vuppaladadiyam AK, Reguyal F, Joshi J, Sharma A, Shah K, Gupta A, Chin BLF, Saptoro A, Sarmah AK. (2024 Jun). Can pyrolysis handle biomedical wastes? Assessing the potential of various biomedical waste treatment technologies in tackling pandemics. *Science of the Total Environment*. *946*, 174167. https://doi.org/10.1016/j.scitotenv.2024.174167
32. Tobiszewski M, Namieśnik J. (2012 Mar). PAH diagnostic ratios for the identification of pollution emission sources. *Environmental Pollution*. *162*, 110–9. https://doi.org/10.1016/j.envpol.2011.10.025
33. U.S. Environmental Protection Agency. *National Primary Drinking Water Regulations. Washington* (DC): U.S. Environmental Protection Agency. https://www.epa.gov/ground-water-and-drinking-water/national-primary-drinking-water-regulations
34. United States Environmental Protection Agency. (2024 Dec 19). *National recommended water quality criteria – human health criteria table.* Washington (DC): Office of Water, U.S. EPA; https://www.epa.gov/wqc/national-recommended-water-quality-criteria-human-health-criteria-table
35. Verbruggen EMJ. (2012). *Environmental risk limits for polycyclic aromatic hydrocarbons (PAHs): For direct aquatic, benthic, and terrestrial toxicity*. RIVM Report 607711007/2012. Bilthoven (NL): National Institute for Public Health and the

Environment (RIVM); https://www.rivm.nl/bibliotheek/rapporten/607711007.pdf

36. World Health Organization. (2022). *Guidelines for drinking-water quality: Fourth edition incorporating the first and second addenda*. Geneva: World Health Organization; 668. https://www.who.int/publications/i/item/9789240045064
37. Xu K, Gao D, Lin J, Dai Q, Zhou Q, Chen Y, Wang C. (2023 May). Benzo[a]pyrene exposure in early life suppresses spermatogenesis in adult male zebrafish and is associated with methylation of germ cell-specific genes. *Aquatic Toxicology*. 258:106504. https://doi.org/10.1016/j.aquatox.2023.106504
38. Zaki SR, Al Obaidy AHMJ, Meshjel MH. (2025). Ecological risk assessment of polycyclic aromatic hydrocarbons (PAH) in the Tigris River water in Baghdad and Wasit cities, Iraq. *IOP Conference Series: Earth and Environmental Science*. 1487, 012004. https://doi.org/10.1088/1755-1315/1487/1/012004
39. Zhang Y, Yuan L, He S, Tao H, Xie W, Zhang X, et al. (2022 Feb 27). Contemporary Research Progress on the Detection of Polycyclic Aromatic Hydrocarbons. *International Journal of Environmental Research and Public Health*. *19*(5), 2790. https://doi.org/10.3390/ijerph19052790
40. Zhao Z, Gong X, Zhang L, Yao S, Xue B. (2022 Jun). North–South geographic heterogeneity and control strategies for polycyclic aromatic hydrocarbons (PAHs) in Chinese lake sediments illustrated by forward and backward source apportionments. *Journal of Hazardous Materials*. 431, 128545. https://doi.org/10.1016/j.jhazmat.2022.128545